TECHNICAL REPORT ARCCB-TR-00012

X-RAY DIGITAL IMAGE PLATE
DETECTOR FOR PHASE AND TEXTURE
ANALYSES OF THIN TANTALUM FILMS

D. WINDOVER
E. BARNAT
J. SUMMERS
T.-M. LU
S.L. LEE

JULY 2000

**US ARMY ARMAMENT RESEARCH,
DEVELOPMENT AND ENGINEERING CENTER**
CLOSE COMBAT ARMAMENTS CENTER
BENÉT LABORATORIES
WATERVLIET, N.Y. 12189-4050

BENÉT LABS

APPROVED FOR PUBLIC RELEASE; DISTRIBUTION UNLIMITED

20000818 137

DISCLAIMER

The findings in this report are not to be construed as an official Department of the Army position unless so designated by other authorized documents.

The use of trade name(s) and/or manufacturer(s) does not constitute an official endorsement or approval.

DESTRUCTION NOTICE

For classified documents, follow the procedures in DoD 5200.22-M, Industrial Security Manual, Section II-19, or DoD 5200.1-R, Information Security Program Regulation, Chapter IX.

For unclassified, limited documents, destroy by any method that will prevent disclosure of contents or reconstruction of the document.

For unclassified, unlimited documents, destroy when the report is no longer needed. Do not return it to the originator.

REPORT DOCUMENTATION PAGE

| 1. AGENCY USE ONLY (Leave blank) | 2. REPORT DATE
July 2000 | 3. REPORT TYPE AND DATES COVERED
Final |
|---|---|---|

4. TITLE AND SUBTITLE

X-RAY DIGITAL IMAGE PLATE DETECTOR FOR PHASE
AND TEXTURE ANALYSES OF THIN TANTALUM FILMS

5. FUNDING NUMBERS

AMCMS No. 6111.01.91A1.1

6. AUTHOR(S)

D. Windover (Benet and RPI, Troy, NY), E. Barnat (RPI),
J. Summers (RPI), T.-M. Lu (RPI), and S.L. Lee

7. PERFORMING ORGANIZATION NAME(S) AND ADDRESS(ES)

U.S. Army ARDEC
Benet Laboratories, AMSTA-AR-CCB-O
Watervliet, NY 12189-4050

8. PERFORMING ORGANIZATION REPORT NUMBER

ARCCB-TR-00012

9. SPONSORING/MONITORING AGENCY NAME(S) AND ADDRESS(ES)

U.S. Army ARDEC
Close Combat Armaments Center
Picatinny Arsenal, NJ 07806-5000

10. SPONSORING/MONITORING AGENCY REPORT NUMBER

11. SUPPLEMENTARY NOTES

12a. DISTRIBUTION/AVAILABILITY STATEMENT

Approved for public release; distribution unlimited.

12b. DISTRIBUTION CODE

13. ABSTRACT (Maximum 200 words)

An x-ray digital image plate detector was used to conduct phase and texture analyses of thin tantalum films in several seconds using a conventional, fixed copper anode, x-ray tube. This plate imaging method provides an expansion of grazing-incidence x-ray diffraction, out of the goniometer plane. The method exploits Laue flat plate geometries and "tall" Debye-Scherrer camera methods. The film studied shows 200-nm of sputter-deposited, α-phase tantalum, showing <110> fiber texture grown on a silicon (100) substrate. Image plate texture information was presented, and confirmed through comparison with conventional pole figure and 2θ Bragg analyses.

14. SUBJECT TERMS

Image Plate, Digital Films, Tantalum, Phase, Texture

15. NUMBER OF PAGES

11

16. PRICE CODE

17. SECURITY CLASSIFICATION OF REPORT	18. SECURITY CLASSIFICATION OF THIS PAGE	19. SECURITY CLASSIFICATION OF ABSTRACT	20. LIMITATION OF ABSTRACT
UNCLASSIFIED	UNCLASSIFIED	UNCLASSIFIED	UL

TABLE OF CONTENTS

LIST OF ILLUSTRATIONS

ACKNOWLEDGEMENTS

INTRODUCTION

The determination of crystal structure and texture has been an important aspect of x-ray analysis since its inception. The uses for texture information pervade every industrial material application; from rolling fiber textures in steel and aluminum production in general manufacturing, to high-wear stabilized coatings in the military, to heteroepitaxial and polycrystalline conducting film textures in semiconductor microelectronics (ref 1). However, the methods for texture analysis using conventional x-ray pole figure and θ-2θ, Bragg-type analyses have remained relatively unchanged over the past thirty years.

Through the advancement of fast computer analysis, several promising two-dimensional detection schemes (refs 2,3) now provide faster collection of texture information. Of these detectors, the digital image plate technique is seen to be very effective at neutron Laue images (ref 4), and x-ray synchrotron crystal truncation rod images (ref 5). In this report, we demonstrate that the digital image plate technique can be used as a fast x-ray imaging system for the study of film texture and crystal phase using a conventional, copper anode x-ray source.

EXPERIMENTAL METHOD

To make an image, a europium ion trapped in a phosphor matrix is excited to a metastable state by an incident x-ray. This excited state is then harmonically released by a laser, during a scanning process, to produce a latent phosphor image, that is then transferred digitally to a computer by a scanner. This phosphor image provides a dynamic range over seven orders of magnitude. Current scanning techniques limit an effective dynamic range to five orders of magnitude. This texture technique can work equally well for any of the current or future two-dimensional detector array schemes. Flat plate geometries have been exploited to provide compatibility for the planar limitations of competitive detection systems.

Recently, reflection high-energy electron diffraction has been able to provide surface configuration and texture information by the reflection of a wavelength of ~0.1-nm electron providing Bragg reflections from a film surface (ref 6). This grazing-incidence geometry is similar to our current x-ray image plate system, so the patterns between the two techniques should be similar. Litvinov and Clarke (ref 7) have postulated a fiber texture model for reflection high-energy electron diffraction patterns. This model has been applied to our texture, and the model fit is presented for comparison.

Tantalum is a high melting point material, which has applications as a refractory coating (ref 8) and as a diffusion barrier in microelectronics (ref 9). In tantalum thin-film formation, an α-, thermally-stable, body-centered-cubic phase (ref 10) and a β-, metastable tetragonal phase of the material may form based on minute changes in the deposition process. Conventional pole figure analysis is rather slow, taking tens of minutes to hours for a complete pole figure with measurement speed depending on the thickness of the film. The 2θ scans, although much quicker, and capable of even faster measurement using a linear array detector, can typically isolate phase information, but can be inconclusive about texture information. A two-dimensional detector can collect enough information to provide both phase and texture information in a very short time.

RESULTS

In our study, an α-phase tantalum film was imaged using an image plate detector, and conventional texture analysis was performed to confirm plate results. The χ-angle discussed is the equivalent of the χ-angle used in pole figures. In the plate geometry, χ is the angle measured from a horizontal line, drawn through the primary beam (region (a) in Figure 1), and tilted up and down using the location of the primary beam as the (0,0) coordinate. One can think of χ-rotation as pinning the plate primary beam and manually rotating the image. Figure 1 shows a plate image taken at a grazing x-ray incident angle of 10° for three seconds on a 200-nm sputter-deposited tantalum film with a silicon (100) substrate. A conventional copper anode x-ray source, operating at 40 kV and 40 mA was collimated using a 1-mm-round source orifice near the tube (~24-mm from the source) and a 0.5-mm refining orifice located close to the sample (~20-mm from the source). The entire source-to-sample path was 286-mm. The 0.4×12-mm x-ray tube was rotated 90° to provide an approximately 1.2×4-mm point source.

The pattern of sharp, high-intensity, concentric streaks, seen in Figure 1, represents a three-dimensional picture of the silicon substrate reciprocal-space lattice collapsed onto a two-dimensional image. This information must be separated from the film information. The symmetric nature of these streaks indicates that the silicon substrate was rotated to a principal axis with respect to the incident x-ray beam. Rotating the single crystal in the pole figure geometry φ direction (rotating the sample around an axis perpendicular to the surface normal) produces asymmetric silicon patterns.

The diffuse rings in the figure represent a Debye-Scherrer image of the (110), (200), and (211) tantalum reflection cones. The bright dot to the left above region (a) is the primary beam intersection with the plate. The three distinct darker regions, labeled (b), are the tantalum (110) family of planes. The two dark regions, labeled (c), are from the (200) family of planes. A third set of planes, the (211), is labeled (d). The (110) tantalum ring shows sharp intensity at 0° and ±60°. This corresponds to intersection reflections at [110]‖(101) at $\chi = 60°$, [110]‖(110) at $\chi = 0°$, and [110]‖(011) at $\chi = -60°$. The (200) ring shows intensity at ±45°, which gives: [110]‖(200) at $\chi = 45°$ and [110]‖(020) at $\chi = -45°$. Similarly, the (211) reflection plane provides [110]‖(211) at $\chi = 30°$ and [110]‖(121) at $\chi = -30°$ and weak, second-order intersections of [110]‖(2-11) at $\chi = 73°$ and [110]‖(-121) at $\chi = -73°$. These angles correspond to tabulated interplaner angles predicted for <110> fiber crystal structure (ref 11). We see the <110> orientation and α-phase in three seconds. We can see the χ-angle (crystal reflection plane tilt angle with respect to the substrate normal) from a pole figure easily, but not the φ-angle (crystal reflection plane rotation angle with respect to the substrate reference frame).

Figure 2 shows a model fit for the <110> fiber texture. The model assumes a fiber crystal structure orientated perpendicular to the surface. The simulation can be applied to any fiber texture and can be set to account for fiber texture that is tilted from the substrate. We found the fit quite acceptable for this <110> fiber. The point at region (a) corresponds to the long, drawn diffuse region (in Figure 1 directly above (a)) that corresponds to the specular reflection from the surface. Region (b) corresponds to the (101), (110), and (011) reflection planes at $\chi = 60°, 0°, -60°$. Region (c) indicates reflections from (200) and (020) at $\chi = 45°, -45°$. Region (d)

2

exhibits (2-11), (211), (121), (-121) reflections at $\chi = 73°, 30°, -30°, 73°$, respectively. The units on the plot are in lattice parameter a values, 0.33-nm for tantalum. This would need to be scaled to Figure 1, and corrected for a slight tilt in the plate image.

Figure 3a shows χ data from a conventional (110) plane pole figure for the same sample and compares these data to Figure 3b, the integrated measurements of Figure 1, measured at different χ angles—$\Delta\chi = 5°$ from 0° to 80°. One complication in our system is that our plates are mounted at 80° from the primary beam instead of 90°. A cosine correction had to be applied to image angles to compare them directly. Another complication is that pole figures, due to the nature of tilting the substrate during a scan, need to be corrected for defocusing errors. The plate method is free from this problem. Both sets of data are shown uncorrected to show the difference in intensities that is caused by defocusing in the pole figure. Region 1 in Figures 3a and 3b corresponds to the primary intersection reflection [110]∥(110). Region 2, located around 60°, corresponds to a mixed distribution of (101) and (011) intersections characteristic of a <110> fiber texture.

To confirm the previous interpretations of data, conventional pole figure analysis was performed on the sample used in Figure 1. The (110), (200), and (211) pole figures were analyzed using the same copper x-ray source. A $2° \times 2°$ tilt and rotation increment was chosen with a three-second collection time at each point. Due to the presence of high-intensity silicon substrate peaks, no background collection was performed and no correction tables were applied to pole figures. Each pole figure analysis took approximately three hours. Figure 3c shows the (110) pole figure for tantalum with a central peak at 0° and a ring for [110] intersecting (101) and (011) at 60°. This (110) pole figure shows a classic <110> fiber texture. Pole figures of the (200) and (211) reflections showed similar <110> fiber texture confirmation and are not shown or discussed in detail in the interest of brevity. One interesting result was found with the tantalum (200) pole figure collected at 55.55° 2θ. This pole figure was overlapping the silicon (311) located at 56.122°, causing a mixture of poles and fiber information that was difficult to interpret. A distinct advantage with image plate information is the ability to qualitatively recognize contributions from substrates in the pattern. This type of visual aid is not available in pole figures and makes separating film data from substrate data difficult.

For complete confirmation of our texture and phase analysis, a grazing-incidence scan with a fixed incidence angle of 10°, Figure 4a, and a conventional θ-2θ Bragg diffraction scan, Figure 4b, were performed on the sample from Figure 1. These scans were conducted using copper radiation at 40 kV and 35 mA, and took approximately 30 minutes per scan. Both scans show the prominent (110) reflection expected for a <110> fiber texture. The stronger signal intensities in the conventional scan, Figure 4b, show the benefits of the Bragg-Brentano focusing geometry. However, the unusually high "(211) tantalum" peak in the conventional scan will have contributions from a close silicon substrate peak. The presence of a (002) β-phase tantalum is beyond the scope of this report and will be discussed formally in a future work.

CONCLUSION

In conclusion, the image plate <110> texture analysis has been confirmed using conventional pole figures and x-ray diffraction scans. A model has been shown to quickly provide interpretation of plate images directly. The technique can also provide comparable χ-scan pole figure data without the defocusing errors present in pole figure collection schemes. In summary, we show that this imaging technique can provide quick analysis for fiber systems and can provide texture and phase information on the scale of seconds.

REFERENCES

1. Mello, K.E., Murarka, S.P., Lu, T.-M., and Lee, S.L., *Journal of Applied Physics*, Vol. 81, 1997, p. 7261.

2. Bunge, H.J., and Klein, H., *Zeitschrift fuer Metallkunde*, Vol. 87, 1996, p. 465.

3. Thomas, M., and von Seggern, H., *Journal of Applied Physics*, Vol. 81, 1997, p. 5887.

4. Niimura, N., Minezaki, Y., Nonaka, T., Castagna, J.-C., Cipriani, F., Høghøj, P., Lehmann, M.S., and Wilkinson, C., *Nature Structural Biology*, Vol. 4, 1997, p. 909.

5. Shimura T., and Havada, J., *Journal of Applied Crystallography*, Vol. 26, 1993, p. 151.

6. Litvinov D., and Clarke, R., *Applied Physics Letters*, Vol. 74, 1999, p. 955.

7. Litvinov, D., O'Donnell, T., and Clarke, R., *Journal of Applied Physics*, Vol. 85, 1999, p. 2151.

8. Lee S.L., and Windover, D., *Surface and Coatings Technology*, Vol. 108-9, 1998, p. 65.

9. Ono, H., Nakano, T., and Ohta, T., *Applied Physics Letters*, Vol. 64, 1994, p. 1511; also Holloway, K., Fryer, P.M., Cabral, C., Jr., Harper, J.M.E., Bailey, P.J., and Kelleher, K.H., *Journal of Applied Physics*, Vol. 71, 1992, p. 5433.

10. Edwards, J.W., Speiser, R., and Johnston, H.L., *Journal of Applied Physics*, Vol. 22, 1951, p. 424.

11. Cullity B.D., *Elements of X-Ray Diffraction, 2nd Edition*, Addison-Wesley, Reading, MA, 1956, p. 75.
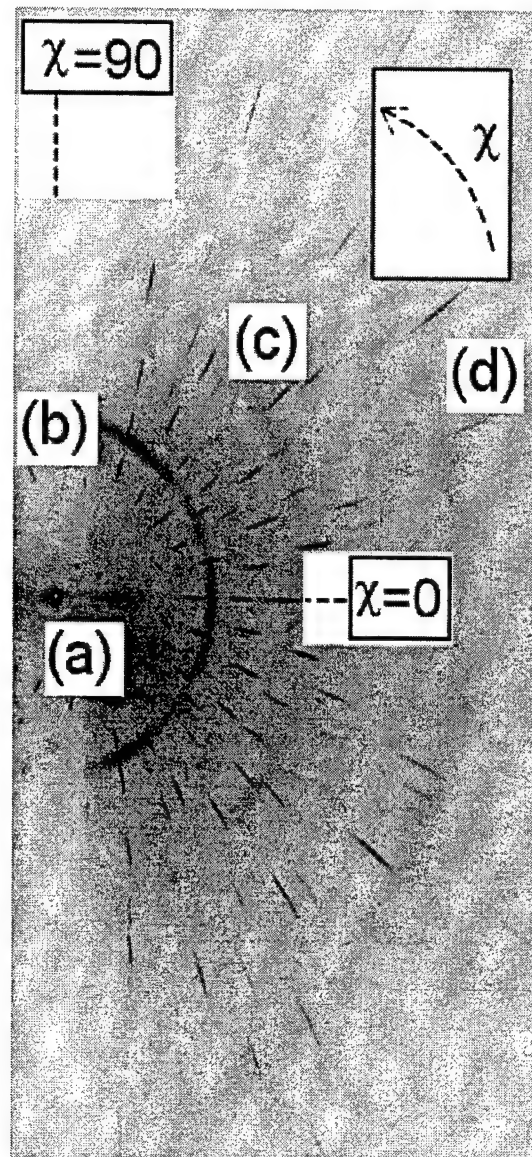
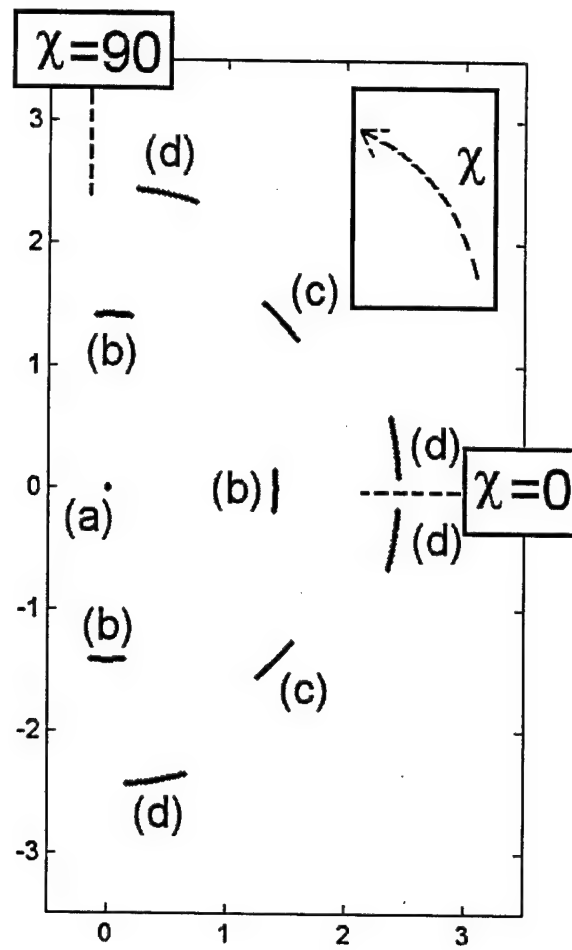Figure 1. Image plate of a 200-nm, <110> fiber texture tantalum on silicon (100) taken for three seconds.

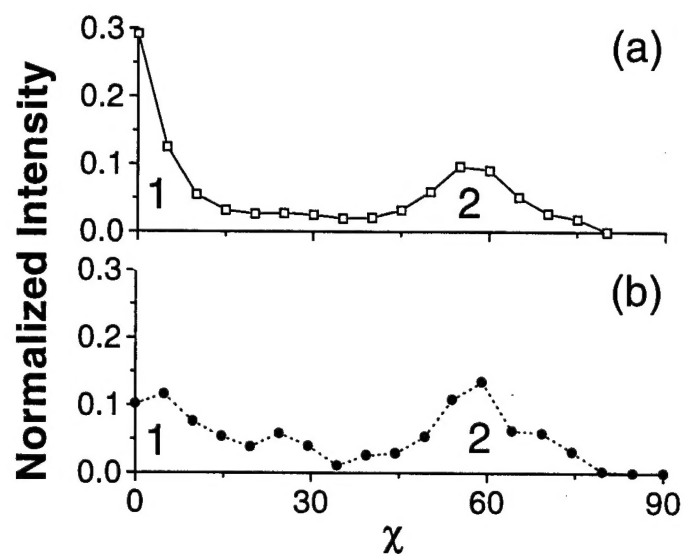Figure 2. Simulation of the <110> fiber texture
produced to compare with Figure 1.

Figures 3a/b. Comparison of (a) χ data from a conventional (110) plane pole figure with (b) integrated measurements of Figure 1.
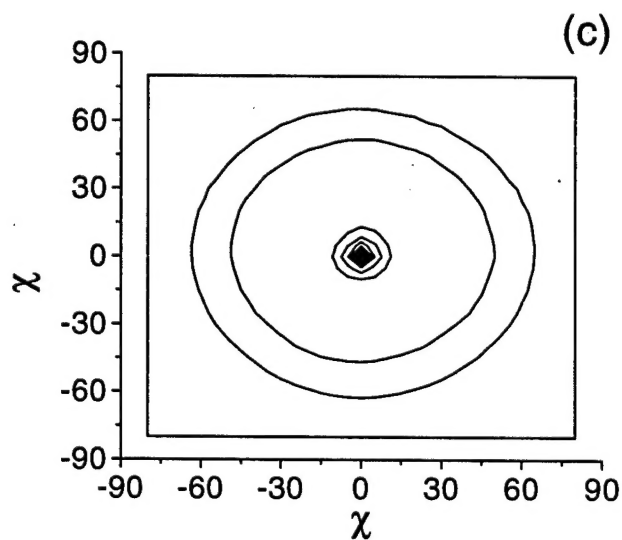

Figure 3c. Conventional (110) plane pole figure showing uniform intensity of texture in the azimuthal, ϕ, direction and $\phi = 0$ data as seen in Figure 3a.
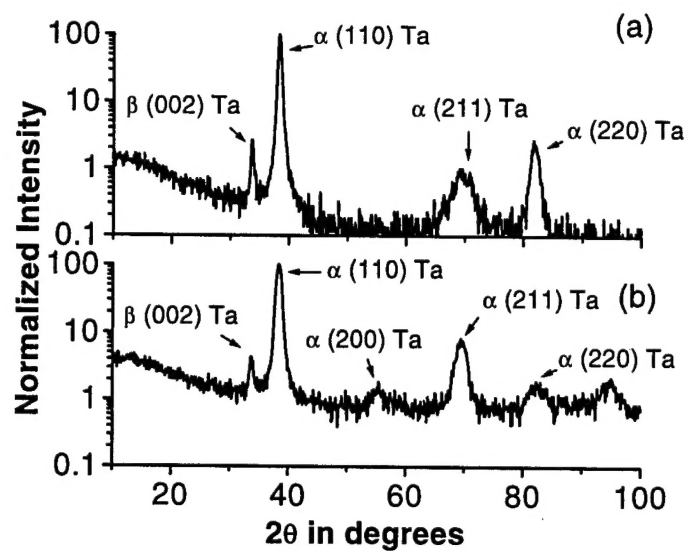
Figure 4. Results of (a) grazing-incidence scan with a fixed incidence angle of 10°, and (b) conventional θ-2θ Bragg diffraction scan, performed on sample from Figure 1.

TECHNICAL REPORT INTERNAL DISTRIBUTION LIST

	NO. OF COPIES
TECHNICAL LIBRARY ATTN: AMSTA-AR-CCB-O	5
TECHNICAL PUBLICATIONS & EDITING SECTION ATTN: AMSTA-AR-CCB-O	3
OPERATIONS DIRECTORATE ATTN: SIOWV-ODP-P	1
DIRECTOR, PROCUREMENT & CONTRACTING DIRECTORATE ATTN: SIOWV-PP	1
DIRECTOR, PRODUCT ASSURANCE & TEST DIRECTORATE ATTN: SIOWV-QA	1

NOTE: PLEASE NOTIFY DIRECTOR, BENÉT LABORATORIES, ATTN: AMSTA-AR-CCB-O OF ADDRESS CHANGES.

TECHNICAL REPORT EXTERNAL DISTRIBUTION LIST

	NO. OF COPIES		NO. OF COPIES
DEFENSE TECHNICAL INFO CENTER ATTN: DTIC-OCA (ACQUISITIONS) 8725 JOHN J. KINGMAN ROAD STE 0944 FT. BELVOIR, VA 22060-6218	2	COMMANDER ROCK ISLAND ARSENAL ATTN: SIORI-SEM-L ROCK ISLAND, IL 61299-5001	1

COMMANDER
U.S. ARMY ARDEC
ATTN: AMSTA-AR-WEE, BLDG. 3022
      AMSTA-AR-AET-O, BLDG. 183
      AMSTA-AR-FSA, BLDG. 61
      AMSTA-AR-FSX
      AMSTA-AR-FSA-M, BLDG. 61 SO
      AMSTA-AR-WEL-TL, BLDG. 59
PICATINNY ARSENAL, NJ 07806-5000
	1
	1
	1
	1
	1
	2
		COMMANDER
		U.S. ARMY TANK-AUTMV R&D COMMAND
		ATTN: AMSTA-DDL (TECH LIBRARY)
		WARREN, MI 48397-5000
			1

DIRECTOR U.S. ARMY RESEARCH LABORATORY ATTN: AMSRL-DD-T, BLDG. 305 ABERDEEN PROVING GROUND, MD 21005-5066	1	COMMANDER U.S. MILITARY ACADEMY ATTN: DEPT OF CIVIL & MECH ENGR WEST POINT, NY 10966-1792	1
DIRECTOR U.S. ARMY RESEARCH LABORATORY ATTN: AMSRL-WM-MB (DR. B. BURNS) ABERDEEN PROVING GROUND, MD 21005-5066	1	U.S. ARMY AVIATION AND MISSILE COM REDSTONE SCIENTIFIC INFO CENTER ATTN: AMSAM-RD-OB-R (DOCUMENTS) REDSTONE ARSENAL, AL 35898-5000	2
COMMANDER U.S. ARMY RESEARCH OFFICE ATTN: TECHNICAL LIBRARIAN P.O. BOX 12211 4300 S. MIAMI BOULEVARD RESEARCH TRIANGLE PARK, NC 27709-2211	1	COMMANDER U.S. ARMY FOREIGN SCI & TECH CENTER ATTN: DRXST-SD 220 7TH STREET, N.E. CHARLOTTESVILLE, VA 22901	1

NOTE: PLEASE NOTIFY COMMANDER, ARMAMENT RESEARCH, DEVELOPMENT, AND ENGINEERING CENTER, BENÉT LABORATORIES, CCAC, U.S. ARMY TANK-AUTOMOTIVE AND ARMAMENTS COMMAND, AMSTA-AR-CCB-O, WATERVLIET, NY 12189-4050 OF ADDRESS CHANGES.